

The cell-permeable mitochondrial calcium uniporter inhibitor Ru265 preserves cortical neuron respiration after lethal oxygen glucose deprivation and reduces hypoxic/ischemic brain injury

Robyn J Novorolsky^{1,2}, Matthew Nichols^{1,2}, Jong S Kim^{3,4}, Evgeny V Pavlov⁵, Joshua J Woods⁶ , Justin J Wilson⁶ and George S Robertson^{1,2,7}

Journal of Cerebral Blood Flow & Metabolism

2020, Vol. 40(6) 1172–1181

© The Author(s) 2020

Article reuse guidelines:

sagepub.com/journals-permissions

DOI: 10.1177/0271678X20908523

journals.sagepub.com/home/jcbfm



Abstract

The mitochondrial calcium (Ca^{2+}) uniporter (MCU) mediates high-capacity mitochondrial Ca^{2+} uptake implicated in ischemic/reperfusion cell death. We have recently shown that inducible MCU ablation in Thyl-expressing neurons renders mice resistant to sensorimotor deficits and forebrain neuron loss in a model of hypoxic/ischemic (HI) brain injury. These findings encouraged us to compare the neuroprotective effects of Ru360 and the recently identified cell permeable MCU inhibitor Ru265. Unlike Ru360, Ru265 (2–10 μM) reached intracellular concentrations in cultured cortical neurons that preserved cell viability, blocked the protease activity of Ca^{2+} -dependent calpains and maintained mitochondrial respiration and glycolysis after a lethal period of oxygen–glucose deprivation (OGD). Intraperitoneal (i.p.) injection of adult male C57Bl/6 mice with Ru265 (3 mg/kg) also suppressed HI-induced sensorimotor deficits and brain injury. However, higher doses of Ru265 (10 and 30 mg/kg, i.p.) produced dose-dependent increases in the frequency and duration of seizure-like behaviours. Ru265 is proposed to promote convulsions by reducing Ca^{2+} buffering and energy production in highly energetic interneurons that suppress brain seizure activity. These findings support the therapeutic potential of MCU inhibition in the treatment of ischemic stroke but also indicate that such clinical translation will require drug delivery strategies which mitigate the pro-convulsant effects of Ru265.

Keywords

Calcium, cerebral ischemia, mitochondria, neuroprotection, motor seizures

Received 26 August 2019; Revised 18 December 2019; Accepted 31 January 2020

¹Department of Pharmacology, Faculty of Medicine, Dalhousie University, Life Sciences Research Institute, Halifax, Canada

²Brain Repair Centre, Faculty of Medicine, Dalhousie University, Life Sciences Research Institute, Halifax, Canada

³Department of Community Health and Epidemiology, Faculty of Medicine, Centre for Clinical Research, Dalhousie University, Halifax, Nova Scotia, Canada

⁴Department of Microbiology, Faculty of Medicine, Centre for Clinical Research, Dalhousie University, Nova Scotia, Canada

⁵Department of Basic Sciences, College of Dentistry, New York University, NY, USA

⁶Department of Chemistry and Chemical Biology, Cornell University, Baker Laboratory, Ithaca, NY, USA

⁷Department of Psychiatry, Faculty of Medicine, Dalhousie University, Life Sciences Research Institute, Halifax, Canada

Corresponding author:

George S Robertson, Life Sciences Research Institute, North Tower, 1348 Summer Street, Halifax B3H 4R2, Canada.

Email: robertgs@dal.ca

Introduction

The MCU mediates high-capacity mitochondrial calcium (Ca^{2+}) uptake.¹ Genetic identification of the MCU in 2011^{2, 3} has enabled the generation of inducible cell-specific MCU deficient mice.^{4, 5} Ablation of the MCU in cardiac myocytes at adulthood protects mice from ischemic/reperfusion injury in the heart.^{4, 5} To determine if neuronal MCU deletion protects mice from hypoxic/ischemic (HI) brain injury, we have recently generated a novel transgenic line enabling tamoxifen-induced MCU deletion in Thy1-expressing neurons.⁶ Relative to Thy1 controls, Thy1-MCU deficient mice were resistant to HI-induced sensorimotor deficits, mitochondrial injury in CA1 hippocampal neurons and neuronal damage in the striatum, dorsal hippocampus and motor cortex.⁶ MCU silencing by siRNA delivery in primary cortical neuron cultures also mitigated OGD-induced respiratory deficits and viability loss.⁶ These findings suggest that the MCU is a novel drug target for ischemic stroke.

The ruthenium coordination compound Ru360 is among the most potent known inhibitors of the MCU.⁷ However, the therapeutic potential of Ru360 is hindered by the poor cell permeability of this MCU inhibitor.⁸ A structural analog of Ru360, termed Ru265, is a cell-permeable MCU inhibitor that prevents loss of the mitochondrial membrane potential (Ψ_m) after hypoxia/reoxygenation in neonatal rat ventricular myocytes by suppressing mitochondrial Ca^{2+} overloading.⁸ The Ψ_m provides the electrochemical driving force for MCU-mediated Ca^{2+} uptake.⁹ Collapse of the Ψ_m therefore impairs mitochondrial Ca^{2+} buffering required to oppose the rise in cytosolic Ca^{2+} concentrations that promote ischemic/reperfusion injury in heart and brain.⁴⁻⁶ This stimulates the Ca^{2+} -activated protease calpain that rapidly destroys the structural integrity of neurons.¹⁰ Calpain inhibitors have broad neuroprotective activities in rodent models of ischemic and hemorrhage stroke, traumatic spinal cord and head injury, multiple sclerosis and Parkinson's disease.¹¹⁻¹⁵

These findings motivated us to compare the cellular uptake and protective effects of Ru360 and Ru265 on cell viability in primary cultures of mouse cortical neurons subjected to a lethal period of OGD. Since Ru265 proved to be the superior MCU inhibitor on these measures, the ability of Ru265 to preserve mitochondrial respiration and glycolysis was assessed next in cortical neurons subjected to OGD. We then examined the dose-dependent effect of Ru265 (3, 10 and 30 mg/kg, i.p.) on the frequency and duration of seizure-like behaviours. Based on the results of these studies, we then measured plasma and forebrain ruthenium concentrations in mice 1 h after an injection of Ru265

(1 or 10 mg/kg, i.p.) to estimate brain penetration by this cell permeable MCU inhibitor. Lastly, the protective effects of a maximally tolerated dose of Ru265 (3 mg/kg, i.p.) were tested in mice subjected to HI brain injury.

Methods

Cortical neuron cultures, Ru265 and Ru360 treatments, cell lysis and protein assay

All studies were conducted according to the guidelines set by the Canadian Council on Animal Care (CCAC) and approved by the University Committee on Laboratory Animals (UCLA) ethics committee at Dalhousie University. Primary cortical cultures derived from C57Bl/6 mice were seeded on 24-well plates at a density of 200,000 neurons/well according to our previously described methods.¹⁶ At 12 days in culture, cortical neurons were exposed to Ru360 (2, 10 or 50 μM) or Ru265 (2, 10 or 50 μM) for 30 min or 24 h. The media was then removed, and the cells were washed three times with 500 μl of ice-cold phosphate-buffered saline (PBS). Next, 75 μl of RIPA cell lysis buffer was added to each well for 30 min. Cell lysates were collected from wells and stored at -80°C until protein concentrations were measured with a Bradford protein assay.

Microwave-assisted digestion

Microwave-assisted digestion was used to digest cell lysates prior to the measurement of Ruthenium (Ru) by ICP-MS; 100 μl of cell lysates were added into 10 ml quartz digestion vessels (CEM Corporation, NC, USA), then 100 μl of concentrated nitric acid (HNO_3 , trace metal grade, Fisher Scientific, ON, Canada) and 800 μl of Milli-Q water (Advantage A10 System, Millipore Corporation, France) were added into the digestion vessel. Samples were digested using a Discovery SPD Microwave Digestor (CEM Corporation, NC, USA) at 165°C , 400 psi and 300 W. Following digestion, the samples were cooled to room temperature in an autosampler rack and then diluted with 4 ml of Milli-Q water to a final sample volume of 5 ml.

Inductively coupled plasma mass spectrometry

Ru concentrations in digested cell lysate samples were quantified using an iCAP Q ICP-MS (Thermo Fisher Scientific, MA, USA) paired with an ESI SC-4DXS autosampler (Elemental Scientific, NE, USA) in Kinetic Energy Discrimination (KED) mode, using high purity helium (99.999%) as the collision gas.

A seven-point calibration curve (0.05, 0.1, 0.5, 1, 5, 10, and 50 $\mu\text{g/l}$ Ru in 2% nitric acid) was used to determine unknown concentrations of Ru in samples. Online internal standard addition was performed to correct for any instrumental drift using 50 $\mu\text{g/l}$ scandium in 2% nitric acid delivered with an SC FAST Valve (Elemental Scientific, NE, USA). A quality control check standard was analyzed every 20 samples. ICP-MS analysis was carried out with a dwell time of 0.01 and 25 sweeps. A minimum of three main runs with a maximum relative standard deviation (SD) of 5.0% were taken for each sample.

MCU inhibitor treatments and cell viability measurements

Primary cortical cultures derived from C57Bl/6 mice were seeded on 48-well plates at a density of 150,000 neurons/well. Cultures (in vitro day 12) were untreated (control) or incubated with Ru360 (10 or 50 μM) or Ru265 (1, 2.5, 5.0, 7.5 or 10 μM) for 30 min or 24 h prior to oxygen–glucose deprivation (OGD; 90 min). Cell viability was examined at 24 h using a 3-(4,5-dimethylthiazol-2-yl)-2,5-diphenyltetrazolium bromide (MTT) assay (Sigma-Aldrich, MO, USA). The effects of treating cortical neurons with Ru265 (10 μM) 5 min after OGD on cell viability were also examined at 24 h using a MTT assay.¹⁶

Assessment of mitochondrial function and glycolysis

The effects of treating cortical neuron cultures with Ru265 (50 μM) for 30 min before OGD (30 min) on oxygen consumption rates (OCRs) and extracellular acidification rates (ECARs) were examined 2 h later as previously described.¹⁶ Control cultures (No OGD) were untreated or incubated with Ru265 (No OGD) for 4 h prior to measuring OCRs and ECARs.

Western blotting

Western blotting was performed as described previously.⁶ Briefly, total protein extracts from primary cortical neuron cultures were separated by SDS-PAGE gel electrophoresis and transferred onto a PVDF membrane. The PVDF membranes were incubated with antibodies against αII -spectrin (AA6 – BML-FG6090, Enzo Life Sciences) and β -actin (A2066, Sigma-Aldrich), washed, incubated with a secondary antibody (anti-mouse IgG PI-2000, Vector; 1:1000) and washed again. An Amersham ECL prime Western blotting detection kit (RPN 2232, GE healthcare) was then applied to the membrane immediately before imaging on a ChemiDoc Touch (BioRad). Images were then exported into Image J, where relative areas for each band were calculated. The ratio of the intact and

calpain-cleaved αII -spectrin to the β -actin signal was calculated and these values were used to calculate a relative expression for each lane.⁶

Measurements of seizure-like behaviours

Three groups, each composed of four adult (20 g; 12 weeks old) male C57/Bl6 mice, were given an intraperitoneal (i.p.) injection of Ru265 dissolved in saline at a dose of either 3 or 10 or 30 mg/kg. Animals were then observed for 90 min (min) by two raters unaware of the treatment conditions. The frequency of seizure-like behaviours including whisker trembling, motionless staring, facial jerking, mild clonic seizures in the sitting and on belly position and severe clonic seizures (convulsions lasting 15 min or more) was measured using a revised Racine scale for mice.¹⁷ The durations of clonic seizures were also measured during the 90-min test period.

Measurement of Ru concentrations in plasma and forebrain

Three groups, composed of four adult (20 g; 12 weeks old) male C57/Bl6 mice each, were injected with either saline (8 ml/kg, i.p.) or Ru265 (1 mg/kg, i.p.) or Ru265 (10 mg/kg, i.p.). One hour later, all animals were injected with an overdose of pentobarbital (150 mg/kg, i.p.) and peripheral blood collected by cardiac puncture. The animals were then perfused intracardially with 10 ml of normal saline to remove the blood from the brain. Forebrains were then harvested and dried at 99°C for 16 h. Each blood sample was transferred to a Microtainer[®] plasma separator tube containing lithium heparin (BD, Franklin Lakes, NJ) and centrifuged at 10,000 $\times g$ for 2 min at room temperature. Plasma was collected and immediately stored at -80°C . Plasma (500 μl) and dried forebrains were then placed in 3 ml of 70% nitric acid and homogenized in a microwave homogenizer. Both blood and forebrain samples were then diluted to a working nitric acid solution of 2% and analyzed by ICP-MS to measure ruthenium concentrations. Since each Ru265 molecule contains two ruthenium atoms, Ru values were divided by half to estimate Ru265 concentrations. Forebrain concentrations were estimated from dry weight by multiplying the ratio of wet to dry weight with 1 g of brain equalling 1 ml of water.

HI brain damage

Two groups, each composed of 8 adult (20 g; 12 weeks old) male C57Bl/6 mice, were injected with saline (8 ml/kg, i.p.) or Ru265 (3 mg/kg, i.p.) and subjected to HI brain injury 30 min later as described previously.¹⁶ In brief, the left common carotid artery was

occluded and then the mice were placed in an 8% oxygen chamber for 50 min to produce a unilateral infarct. Animals were injected with an over-dose of pentobarbital (150 mg/kg, i.p.) and perfused with PBS 24 h later. Brains were then removed and 5 coronal sections (1 mm thick) spanning 1.5 to -2.5 mm (anterior to posterior) from bregma were stained with 2,3,5-triphenyltetrazolium chloride (TTC; Sigma-Aldrich) staining. TTC staining and quantification were done in a single-blinded fashion to calculate the infarct volumes in the affected hemisphere in accordance with the ARRIVE guidelines.^{6,16,18}

Neuroscore scale: Assessment of general condition and neurological deficits

A comprehensive behavioural assessment of sensorimotor deficits produced by HI brain injury was performed using a neuroscore scale developed by Dr. Ulrich Dirnagl (Charité - Universitätsmedizin Berlin, Germany). Scores ranged from 0 (healthy) to 56 (the worst performance in all categories) and represented the sum of scores for six general deficit categories (hair, ears, eyes, posture, spontaneous activity and epileptic behaviour categories) and seven focal deficits categories (body symmetry, gait, climbing on angled surface, circling behaviour, front limb symmetry, compulsory circling, whisper response to light touch). A full description of these methods is available in Nichols et al.¹⁶

Power calculations and statistical analyses

Power calculations were performed using G*Power 3.1 statistical software to determine the group sizes required to detect differences for the animal experimentation. A group size of eight mice was needed to detect a 30% difference between two means with a standard error of 25% at a power (1- β) of 0.8 for measurements of neuroscores and infarct volumes at an alpha level of 0.05 using the Mann-Whitney U test. A one-way ANOVA (Kruskal-Wallis) followed by Dunn's test was used to compare the effects of increasing concentrations of Ru265 on cell viability after OGD. These statistical tests were also used to compare the effects of pre- (24 h and 30 min) and post (5 min)-treatments with Ru265 on protection against OGD-induced cell viability loss. A two-way ANOVA followed by group comparisons with the Bonferroni's post hoc test was used to assess potential differences between control and Ru265-treated cortical neuron OCRs and ECARs. The half-maximal effective concentration (EC_{50}) of Ru265 for increasing cell viability after OGD was calculated using the log (agonist) versus response - Variable slope (four parameters) function for

GraphPad Prism 8.1.2. Infarct volumes were compared with a Mann-Whitney U test. All statistical tests were performed using GraphPad Prism 8.1.2.

Results and discussion

Superior cellular uptake of Ru265 relative to Ru360 in primary cortical neuron cultures

Primary cultures of mouse cortical neurons were incubated with Ru265 or Ru360 at 2, 10 or 50 μ M for 30 min or 24 h (Figure 1(a) and (b)). Mass cellular uptake of Ru265 and Ru360 was estimated by measuring concentrations of ruthenium (Ru) yielded by cell lysis. The limit of detection for Ru using our ICP-MS methodologies was excellent at 0.4 parts/trillion. Since Ru360 and Ru265 each have two Ru atoms, compound concentrations were considered half of the Ru values and shown as nanograms (ng) of Ru/ μ g of protein. Ru265 produced concentration- and time-dependent increases in intracellular Ru levels that were progressively greater than those generated by Ru360 at the equivalent concentrations (2, 10 and 50 μ M) and time points (30 min and 24 h; Figure 1(c) and (d)). Assuming protein and water respectively account for about 20% and 70% of cortical neuron mass, we estimate that exposure of cortical neurons to Ru265 (10 μ M) for 30 min generated intracellular concentrations that approached 100 nM. These findings both confirm and extend previous published data demonstrating the superior uptake of Ru265 over Ru360 in HeLa and HEK293 cells.⁸ However, by comparison to HeLa (65 pg/ μ g protein) and HEK293 (85 pg/ μ g protein) cells treated with Ru265 (50 μ M) for 24 h,⁸ intracellular Ru concentrations were over 90 times higher in cortical neurons (8 ng/ μ g protein). It is possible that methodological differences may have accounted for these discrepant findings. Alternatively, the high metabolic demands imposed by excitatory neurotransmission in cortical neurons after 12 days in culture¹⁹ may have enhanced Ru265 uptake by multiple mechanisms other than entry via the MCU such as organic anion transporters, calcium exchangers and voltage-gated calcium channels.²⁰⁻²² The supra-linear increases in intracellular Ru concentrations generated by Ru265 (10 μ M) over Ru360 (10 μ M) from 30 min to 24 h clearly suggest alternate uptake mechanisms for Ru265 (Figure 1(c) and (d)).

Ru265 produces a concentration-dependent protection of cortical neurons against OGD

Cell viability remained constant in cortical neuron cultures treated with 10 μ M of Ru265 for 72 h (Suppl. Figure 1(a)). Addition of Ru265 to cortical cultures

protects neurons if present during OGD, our findings also provide a potential explanation for the repeated failure of putative neuroprotectants in the clinic.²³

Ru265 blocks calpain activation in cortical neurons subjected to OGD

The excessive rise in cytosolic Ca^{2+} concentrations that occurs during ischemia allosterically increases the cysteinyl protease activity of calpains.²⁴ These Ca^{2+} -dependent proteases destroy the integrity of neurons by degrading structural proteins such as α II-spectrin.¹⁰ We therefore examined the ability of Ru265 to block the cleavage of α II-spectrin by calpain. Western

blotting revealed that levels of calpain-cleaved α II-spectrin were elevated 3, 6 and 24 h after OGD. Incubation with Ru265 (10 μ M) 30 min before OGD suppressed the generation of calpain-cleaved α II-spectrin 3, 6 and 24 h after OGD (Figure 1(g)). These findings indicate that excessive MCU-mediated mitochondrial Ca^{2+} uptake drives injurious calpain activity implicated in ischemic/reperfusion brain damage.^{12,25}

Ru265 preserves mitochondrial respiration and glycolysis in OGD-treated cortical neurons

We next determined whether Ru265 preserved mitochondrial function and glycolysis after OGD.

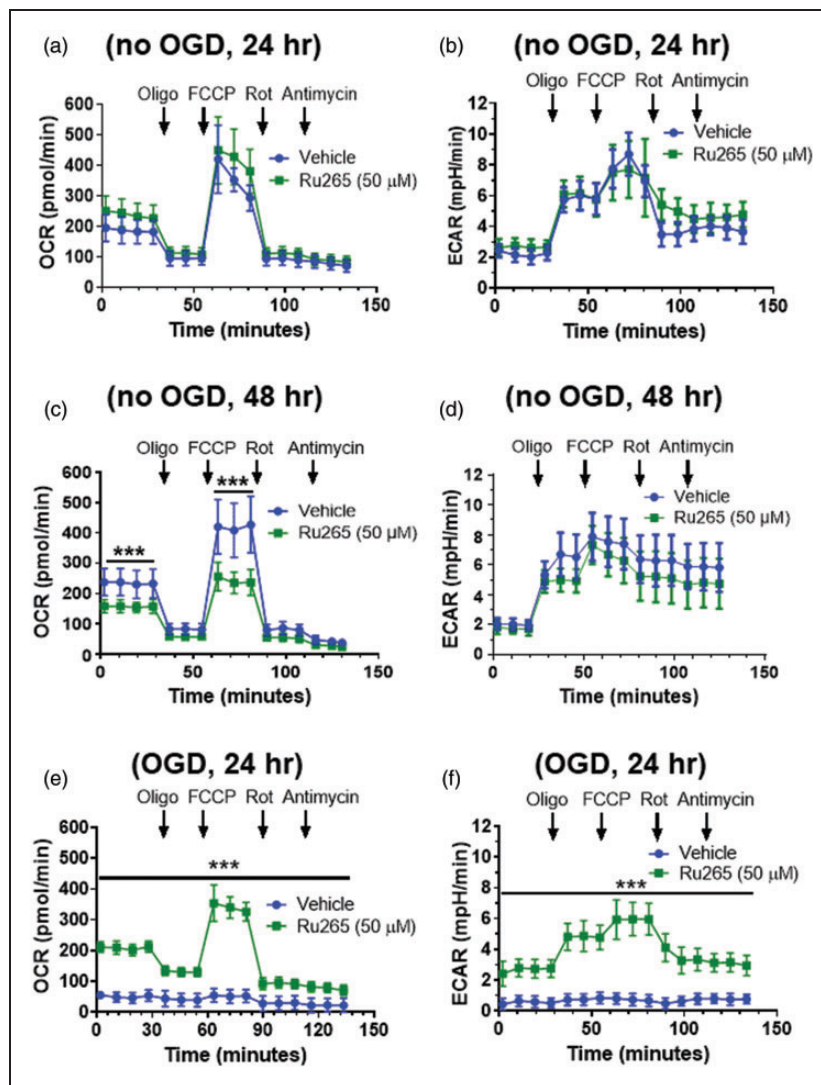


Figure 2. Oxygen consumption rate (OCR) and extracellular acidification rate (ECAR) measurements in primary cortical neurons cultures after the sequentially addition of oligomycin (1 μ M), FCCP (2 μ M), rotenone (300 nM) and antimycin (1 μ M) following treat with Ru265 (50 μ M) for 24 h (a and b) or 48 h (c and d). Pretreatment with Ru265 (50 μ M) for 30 min preserves OCR and ECAR 2 h after 30 min of OGD (e and f). Bars show the mean \pm SD of data representative of three separate experiments. * $p < 0.05$, ** $p < 0.01$ and *** $p < 0.001$, two-way ANOVA followed by Bonferroni's post hoc test.

Pilot experiments indicated that a higher concentration of Ru265 (50 μ M) was required to protect cortical neuron cultures on the XF24 plates than the 48-well polystyrene cell culture plates from viability loss after OGD (data not shown). Pretreatment of control (No OGD) cultures with Ru265 (50 μ M) for 24 h did not alter either basal respiration, maximal respiration induced carbonyl cyanide-4-(trifluoromethoxy) phenylhydrazine (FCCP) or residual respiration (protein leak) observed after the sequential addition of rotenone and antimycin (Figure 2(a)). ECAR, indicative of glycolysis, was also unchanged by pretreatment with Ru265 (50 μ M) for 24 h. However, OCR and ECAR values were suppressed by treatment with Ru265 (50 μ M) for 48 h (Figure 2(c) and (d)). Cell viability was slightly reduced at this time point (15%) with future reductions at 72 h (25%; Suppl. Figure 1(b)). In cultures exposed to OGD (30 min), OCR and ECAR were markedly suppressed (Figure 2(e) and

(f)). Consistent with increased cortical neuron viability after OGD, Ru265 completely preserved mitochondrial respiration and glycolysis 2 h after OGD (Figure 2(e) and (f)). However, ATP production, as defined by OCR values after the addition of oligomycin (2 μ M), was modestly suppressed (30%) in Ru265-treated cortical neurons after OGD relative to control (no OGD) cultures (Figure 2(a) and (e)). These findings indicate that MCU-mediated mitochondrial Ca^{2+} overloading is a pivotal pathological event in the collapse of mitochondrial function after OGD.

Dose-dependent increases in seizure-like behaviours by Ru265

In view of evidence that the systemic injection of ruthenium red, which contains Ru360, produces dose-dependent increases in seizure-like behaviours in rodents and cats,^{26–28} we examined the

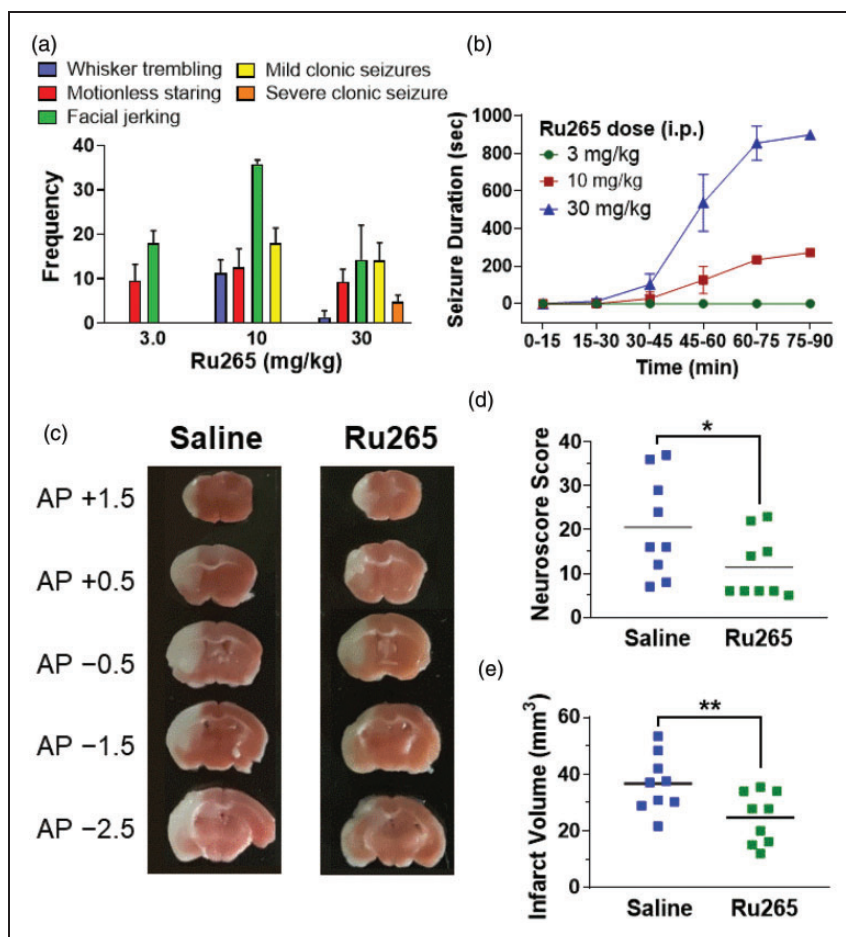


Figure 3. Frequency of seizure-like behaviours detected 90 min after the injection of 3, 10 or 30 mg/kg (i.p.) of Ru265 (mean \pm SD; $n = 4$ /group; a). Durations of clonic seizures detected over a 90-min test period after the injection of 3, 10 or 30 mg/kg (i.p.) of Ru265 (b). Representative TTC stained sections 24 h after HI brain injury for mice injected with saline (8 ml/kg, i.p.) or Ru265 (3 mg/kg, i.p.) 30 min after HI (c). Neuroscores and infarct volumes in mice injected with saline (8 ml/kg, i.p.) or Ru265 (3 mg/kg, i.p.) 24 h after HI brain injury (d and e). * $p < 0.05$ and ** $p < 0.01$, Mann–Whitney U tests.

pro-convulsant effects of Ru265 in adult (20 g) male C57/Bl6 mice. At a dose of 3 mg/kg (i.p.), Ru265 caused bouts of motionless staring, typical of absence seizures,¹⁷ within 30 min of injection that occurred at regular intervals for the remaining 60-min test period (Figure 3(a)). The frequency of motionless staring did not increase at doses of 10 or 30 mg/kg (i.p.). Facial jerking was also observed at 3 mg/kg (i.p.) that became more frequent at 10 mg/kg (i.p.) but declined at 30 mg/kg (i.p.) because the animals became incapacitated by severe clonic seizures (Figure 3(b)). By contrast, 3 mg/kg (i.p.) did not produce clonic seizures (Figure 3(a) and (b)). Whisker trembling at a dose of 10 mg/kg (i.p.) of Ru265 was associated with the induction of mild clonic seizures. Ru265 (30 mg/kg; i.p.) produced severe clonic seizures that lasted for 15 min (Figure 3 (b)). The onset of clonic seizures was also more rapid following the i.p. injection of Ru265 at 30 mg/kg (30 min) than 10 mg/kg (45 min). The severity of these seizures increased over time – by 3 and 6 h all animals had to be euthanized in the 30 and 10 mg/kg groups, respectively.

Ru265 reduces hypoxic/ischemic-induced sensorimotor deficits and brain injury

Based on these findings, the maximally tolerate dose of Ru265 was defined at 3 mg/kg (i.p.). Lastly, we examined the neuroprotective potential of Ru265 in an adult mouse model of HI brain injury. Injection of Ru265 (1 and 10 mg/kg, i.p.) produced a dose-dependent elevation of plasma and forebrain Ru concentrations in adult (20 g) male C57Bl/6 mice (Table 1). Relative to HI mice that received saline (8 ml/kg, i.p.) 30 min before HI, Ru265 (3 mg/kg, i.p.) reduced sensorimotor deficits and infarct volumes 24 h after HI (Figure 3(d) to (f)). Interestingly, measurements of forebrain Ru concentrations suggested that even at a dose of 10 mg/kg (i.p.), Ru265 forebrain concentrations ($0.315 \pm 0.007 \mu\text{M}$) were less than 10% of the EC₅₀ ($5 \mu\text{M}$) for elevating the viability of cortical neurons exposed to OGD. However, our uptake studies also suggest that neurons express at least one transport mechanism, and perhaps several, utilised by Ru265 but not Ru360. The high Ca²⁺ transporter, ion

channel, organic anion and MCU activities associated with neurotransmission²⁹ may thus concentrate this compound in the cytosol and mitochondrial matrix of neurons.^{20–22} Forebrain Ru measurements obviously produce pool-dilution effects that underestimate the concentration of Ru265 in neurons. Lastly, the 10-fold higher potency of Ru265 relative to Ru360 at inhibiting MCU activity further shows that only modest increases in cellular uptake would confer markedly improved protection.⁸

Summary and conclusions

We have previously reported that tamoxifen-induced knockdown of the MCU in Thy1-expressing forebrain neurons (layer V cortex, CA1-3 hippocampus) of adult mice reduced sensorimotor deficits and infarct volumes in the HI brain injury model.⁶ The present findings extend these observations by showing that injection of Ru265 (3 mg/kg, i.p.) modestly reduced HI brain injury in mice. However, Ru265 produced dose-dependent increases in seizure-like behaviours at doses of 10 and 30 mg/kg (i.p.). Interestingly, we are not aware of another neuroprotectant with such pro-convulsant activities.

Ruthenium red induces lethal clonic seizures but at lower doses (4.4 mg/kg, i.p.) than Ru265 (10 mg/kg, i.p.). Unlike ruthenium red ($50 \mu\text{M}$) which reduces rat cortical neuron viability by 50% at 24 h,^{30–32} Ru265 ($50 \mu\text{M}$) did not decrease mouse cortical neuron viability at 24 h and produced only a minor cell viability loss (15%) at 48 h (Suppl. Figure 1(b)). These findings suggest that mechanisms other than MCU inhibition account for the neurotoxic actions of ruthenium red. Unlike cortical neuron cultures treated with Ru265 ($50 \mu\text{M}$) for 24 h, exposure to Ru265 ($50 \mu\text{M}$) for 48 h reduced ATP synthesis, maximal respiratory capacity and glycolysis. Cortical neurons are thus susceptible to metabolic collapse with prolonged MCU inhibition. Inhibitory cortical interneurons with vast dendritic arbours that fire over 100 times/s tonically suppress the activity of brain circuits implicated in seizure activity.^{33–35} The prodigious energy demands of these interneurons are thought to render them highly susceptible to metabolic compromise.³⁶ MCU ablation has recently been shown to impair the synchronization of fast cortical networks that could potentially contribute to seizure development.³⁷ These findings suggest that the inhibition of MCU-mediated Ca²⁺ buffering and ATP synthesis by Ru265 may have caused convulsions by metabolically compromising the activity of interneuron populations that restrain cortical seizure circuits.

Given the low brain penetration, modest neuroprotective activities, and narrow therapeutic window of Ru265, further in vivo studies with the HI brain

Table 1. Plasma and forebrain concentrations of Ru265.

Treatment	Plasma	Forebrain
Saline (8 ml/kg, ip)	ND	ND
Ru265 (1 mg/kg, ip)	$0.771 \pm 0.009 \mu\text{M}$	$0.026 \pm 0.004 \mu\text{M}$
Ru265 (10 mg/kg, ip)	$6.123 \pm 0.012 \mu\text{M}$	$0.315 \pm 0.007 \mu\text{M}$

Note: Plasma and forebrain Ru265 concentrations 1 h after the injection of saline (8 mg/kg, i.p.) or Ru265 (1 or 10 mg/kg, i.p.) determined by measuring ruthenium levels with ICP-MS.

model were deemed of minor therapeutic value and thus arguably unethical. Post-dosing and long-term efficacy studies using both male and female mice recommended by STAIRS guidelines to improve clinical translation were therefore not performed.³⁸ Nevertheless, the ability of Ru265 to markedly suppress cortical neuron viability loss, injurious calpain activity and respiratory deficits in the OGD model clearly support the therapeutic potential of MCU inhibition for the treatment of ischemic/reperfusion brain injury.⁸ However, improved drug delivery strategies will be required to increase the therapeutic window for Ru265. For instance, local injection of nanoparticles loaded with Ru265 and decorated with proteins that target hypoxic neurons in the middle cerebral artery immediately after thrombolytic therapy could conceivably mitigate the pro-convulsant and enhance the neuroprotective effects of Ru265.³⁹

Funding

The author(s) disclosed receipt of the following financial support for the research, authorship, and/or publication of this article: This work was supported by funding from the Heart and Stroke Foundation of Canada (G-18-0021605; GSR), Dalhousie University Brain Repair Centre (Knowledge Translation Grant; GSR) and the US National Science Foundation Grant (CHE-1750295; JJW). Joshua J Woods is funded by a Graduate Research Fellowship from the NSF (Grant No DGE-1650441). Robyn J Novorolsky is funded by a CIHR Scholarship through the Canadian Graduate Scholarship (CGS) – Master’s Program.

Declaration of conflicting interests

The author(s) declared no potential conflicts of interest with respect to the research, authorship, and/or publication of this article.

Authors’ contributions

RJN performed the cell viability, Ru265 and Ru360 uptake and Seahorse XF24 studies. Joshua Woods and Justin Wilson generated Ru360 and Ru265 and assisted with preparation of the manuscript. EVP assisted with the preparation of the manuscript. JSK performed the ICP-MS studies. MN performed studies using the HI model. GSR, JSK and RJN performed the statistical analysis and wrote the manuscript.

ORCID iD

Joshua Woods  <https://orcid.org/0000-0002-6213-4093>

Supplementary material

Supplemental material for this article is available online.

References

1. Kirichok Y, Krapivinsky G and Clapham DE. The mitochondrial calcium uniporter is a highly selective ion channel. *Nature* 2004; 427: 360–364.
2. De SD, Raffaello A, Teardo E, et al. A forty-kilodalton protein of the inner membrane is the mitochondrial calcium uniporter. *Nature* 2011; 476: 336–340.
3. Baughman JM, Perocchi F, Girgis HS, et al. Integrative genomics identifies MCU as an essential component of the mitochondrial calcium uniporter. *Nature* 2011; 476: 341–345.
4. Kwong JQ, Lu X, Correll RN, et al. The mitochondrial calcium uniporter selectively matches metabolic output to acute contractile stress in the heart. *Cell Rep* 2015; 12: 15–22.
5. Luongo TS, Lambert JP, Yuan A, et al. The mitochondrial calcium uniporter matches energetic supply with cardiac workload during stress and modulates permeability transition. *Cell Rep* 2015; 12: 23–34.
6. Nichols M, Pavlov EV and Robertson GS. Tamoxifen-induced knockdown of the mitochondrial calcium uniporter in Thy1-expressing neurons protects mice from hypoxic/ischemic brain injury. *Cell Death Dis* 2018; 9: 606.
7. Emerson J, Clarke MJ, Ying WL, et al. The component of “ruthenium red” responsible for inhibition of mitochondrial calcium ion transport. Spectra, electrochemistry, and aquation kinetics. Crystal structure of $\mu\text{-O-}[(\text{HCO}_2)(\text{NH}_3)_4\text{Ru}]_2\text{Cl}_3$. *J Am Chem Soc* 1993; 115: 11799–11805.
8. Woods JJ, Nemani N, Shanmughapriya S, et al. A selective and cell-permeable mitochondrial calcium uniporter (MCU) inhibitor preserves mitochondrial bioenergetics after hypoxia/reoxygenation injury. *ACS Cent Sci* 2019; 5: 153–166.
9. Duchen MR. Mitochondria, calcium-dependent neuronal death and neurodegenerative disease. *Pflugers Arch* 2012; 464: 111–121.
10. Liu J, Liu MC and Wang KK. Calpain in the CNS: from synaptic function to neurotoxicity. *Sci Signal* 2008; 1: re1.
11. Lai TW, Zhang S and Wang YT. Excitotoxicity and stroke: identifying novel targets for neuroprotection. *Prog Neurobiol* 2014; 115: 157–188.
12. Koumura A, Nonaka Y, Hyakkoku K, et al. A novel calpain inhibitor, ((1S)-1((((1S)-1-benzyl-3-cyclopropylamino-2,3-di-oxopropyl)amino)carbonyl)-3-methylbutyl) carbamic acid 5-methoxy-3-oxapentyl ester, protects neuronal cells from cerebral ischemia-induced damage in mice. *Neuroscience* 2008; 157: 309–318.
13. Crocker SJ, Smith PD, Jackson-Lewis V, et al. Inhibition of calpains prevents neuronal and behavioral deficits in an MPTP mouse model of Parkinson’s disease. *J Neurosci* 2003; 23: 4081–4091.
14. Bains M, Cebak JE, Gilmer LK, et al. Pharmacological analysis of the cortical neuronal cytoskeletal protective efficacy of the calpain inhibitor SNJ-1945 in a mouse traumatic brain injury model. *J Neurochem* 2013; 125: 125–132.

15. Trager N, Smith A, Wallace IG, et al. Effects of a novel orally administered calpain inhibitor SNJ-1945 on immunomodulation and neurodegeneration in a murine model of multiple sclerosis. *J Neurochem* 2014; 130: 268–279.
16. Nichols M, Elustondo PA, Warford J, et al. Global ablation of the mitochondrial calcium uniporter increases glycolysis in cortical neurons subjected to energetic stressors. *J Cereb Blood Flow Metab* 2017; 37: 3027–3041.
17. Van EJ, Van DD and De Deyn PP. PTZ-induced seizures in mice require a revised Racine scale. *Epilepsy Behav* 2019; 95: 51–55.
18. Nichols M, Zhang J, Polster BM, et al. Synergistic neuroprotection by epicatechin and quercetin: activation of convergent mitochondrial signaling pathways. *Neuroscience* 2015; 308: 75–94.
19. Zeiger SL, Stankowski JN and McLaughlin B. Assessing neuronal bioenergetic status. *Methods Mol Biol* 2011; 758: 215–235.
20. Charuk JH, Pirraglia CA and Reithmeier RA. Interaction of ruthenium red with Ca²⁺(+)-binding proteins. *Anal Biochem* 1990; 188: 123–131.
21. Tapia R and Velasco I. Ruthenium red as a tool to study calcium channels, neuronal death and the function of neural pathways. *Neurochem Int* 1997; 30: 137–147.
22. Puckett CA, Ernst RJ and Barton JK. Exploring the cellular accumulation of metal complexes. *Dalton Trans* 2010; 39: 1159–1170.
23. Gladstone DJ, Black SE and Hakim AM. Toward wisdom from failure: lessons from neuroprotective stroke trials and new therapeutic directions. *Stroke* 2002; 33: 2123–2136.
24. Strobl S, Fernandez-Catalan C, Braun M, et al. The crystal structure of calcium-free human m-calpain suggests an electrostatic switch mechanism for activation by calcium. *Proc Natl Acad Sci U S A* 2000; 97: 588–592.
25. Bevers MB and Neumar RW. Mechanistic role of calpains in postischemic neurodegeneration. *J Cereb Blood Flow Metab* 2008; 28: 655–673.
26. Tapia R, Meza-Ruiz G, Duran L, et al. Convulsions or flaccid paralysis induced by ruthenium red depending on route of administration. *Brain Res* 1976; 116: 101–109.
27. Tapia R. Antagonism of the ruthenium red-induced paralysis in mice by 4-aminopyridine, guanidine and lanthanum. *Neurosci Lett* 1982; 30: 73–77.
28. Garcia-Ugalde G and Tapia R. Convulsions and wet-dog shakes produced by systemic or intrahippocampal administration of ruthenium red in the rat. *Exp Brain Res* 1991; 86: 633–640.
29. Zsurka G and Kunz WS. Mitochondrial dysfunction and seizures: the neuronal energy crisis. *Lancet Neurol* 2015; 14: 956–966.
30. Velasco I, Moran J and Tapia R. Selective neurotoxicity of ruthenium red in primary cultures. *Neurochem Res* 1995; 20: 599–604.
31. Velasco I and Tapia R. Ruthenium red neurotoxicity and interaction with gangliosides in primary cortical cultures. *J Neurosci Res* 1997; 49: 72–79.
32. Velasco I and Tapia R. Alterations of intracellular calcium homeostasis and mitochondrial function are involved in ruthenium red neurotoxicity in primary cortical cultures. *J Neurosci Res* 2000; 60: 543–551.
33. Marin O. Interneuron dysfunction in psychiatric disorders. *Nat Rev Neurosci* 2012; 13: 107–120.
34. Cammarota M, Losi G, Chiavegato A, et al. Fast spiking interneuron control of seizure propagation in a cortical slice model of focal epilepsy. *J Physiol* 2013; 591: 807–822.
35. Liou JY, Ma H, Wenzel M, et al. Role of inhibitory control in modulating focal seizure spread. *Brain* 2018; 141: 2083–2097.
36. Kann O. The interneuron energy hypothesis: implications for brain disease. *Neurobiol Dis* 2016; 90: 75–85.
37. Bas-Orth C, Schneider J, Lewen A, et al. The mitochondrial calcium uniporter is crucial for the generation of fast cortical network rhythms. *J Cereb Blood Flow Metab* 2019. Epub Ahead of print 13 November 2019. DOI: 10.1177/0271678X19887777.
38. Recommendations for standards regarding preclinical neuroprotective and restorative drug development. *Stroke* 1999; 30: 2752–2758.
39. Rabiei M, Kashanian S, Samavati SS, et al. Active targeting towards and inside the brain based on nanoparticles: a review. *Curr Pharm Biotechnol* 2019. Epub Ahead of print 2 December 2019. DOI: 10.2174/1389201020666191203094057.